

DISSOLUTION OF TUNISIAN PHOSPHATE ORE BY A MIXTURE OF SULFURIC AND PHOSPHORIC ACID: KINETICS STUDY BY MEANS OF DIFFERENTIAL REACTION CALORIMETRY

O. Lachkar-Zamouri ^a, K. Brahim ^{a*}, F. Bennour ^b, I. Khattech ^a

^{a*} Chemistry Department: LR15ES01 Materials, Cristalochimie and Applied Thermodynamics Laboratory, Faculty of Science, Tunis El Manar University, Tunis, Tunisia

^b Direction of Scientific Research, Tunisian Chemical Group, Sfax, Tunisia

(Received 08 August 2018; accepted 14 January 2019)

Abstract

A mixture of phosphoric and sulfuric acid was used to investigate the dissolution kinetics of phosphate ore by Differential Reaction Calorimetry (DRC). The effect of the solid-to-liquid ratio, concentration, stirring speed, particle size and temperature of the reaction is examined. It was established that the dissolution rate increased with stirring speed and particle size. However, rising the solid-to-liquid ratio, temperature and concentration decreased the dissolution rate. It was determined that the dissolution rate fits in the first order of the pseudo-homogeneous reaction model. Two negative values of apparent activation energies were found in the range of 25 to 60°C. The experimental data were tested by graphical and statistical methods and it was found that the following models were best fitted for the experimental data and an empirical equation for the process was developed.

$$-\ln(1-x) = [2,2 E-09((S/L)^{0.75} C^{-0.461} G^{0.447} (SS)^{0.471} \exp(2671/T))]t. T \leq 40^\circ C$$

$$-\ln(1-x) = [2,2 E-09((S/L)^{0.75} C^{-0.461} G^{0.447} (SS)^{0.471} \exp(6959/T))]t. T > 45^\circ C$$

Keywords: Kinetics; Phosphate ores; Differential reaction calorimetry; Shrinking-core model; Activation energy; Isoconversional model

1. Introduction

Phosphate compounds, which are used in many applications and processes, are available in huge quantities in nature, and are commercially important. The composition of natural phosphate (NP) differs from one source to another. The phosphate ores used for manufacturing fertilizers are mainly sedimentary. Sedimentary phosphates are composed of the apatite group with various amounts of accessory minerals such as carbonates, fluorides, silicates, quartz, clays, oxides, metal, etc. [1,2]. Consequently, these phosphates from various sources are predicted to behave differently in the attack processes. According to available statistic data [3], the world production of phosphate rock (26-34 % P₂O₅) has more than tripled during the last fifty years reaching 217 million tons by 2012 [4].

Several studies on the dissolution of synthetic phosphate [5-12] or phosphate ore [13-23] in acid

solutions have been carried out such as phosphoric acid [5, 15-17], succinic acid [18], acetic acid [19], and hydrochloric acid [6, 20-21] to illustrate the kinetics and process mechanism as well as enhancing the yield of the phosphate attack. Nevertheless, phosphate ore dissolution by sulfuric acid remains the most extensively used process [22] and over 90% of the phosphoric acid produced globally is manufactured through the decomposition of phosphate ore with sulfuric acid as an acidulate [23]. The decomposition of phosphate rocks using aqueous sulfuric acid has been studied by several authors [24-31]. Sevim et al. [24] dissolved Turkish mineral phosphate in sulfuric acid at 14–70°C showing that the reaction rate belongs to a solid-to-liquid ratio, temperature and particle size. An Avrami-type equation was used successfully to describe the kinetic study and the activation energy was found to be 29.66 kJ mol⁻¹. In the same context, Olanipenkun et al. [21] in their work on the acidulation of Nigerian

*Corresponding author: brahimkemaies@gmail.com



phosphorite in aqueous solutions of sulfuric acid at a temperature of 60–90°C indicated that diffusion through an ash layer is the controlling step. The activation energy of this dissolution was determined as 17.60 kJ mol⁻¹. A comparable conclusion was obtained for Nigerian phosphorite in a mixture of sulfuric and hydrochloric acids with an activation energy of 13.25 kJ mol⁻¹ [21].

In most cases, the studies have been carried out directly on natural phosphates, making it very difficult to mechanistically and the conclusions are somewhat contradictory. For example, Ben Brahim et al. [16] was determined that the dissolution rate of Tunisian phosphate ore in dilute phosphoric acid solutions can be described by a Vander Sluis model in the rise from temperature 25 to 90°C and showing that the increase in temperature leads to a decrease in the attack and denote that the rate leaching process is controlled by diffusion rather than with activation energy equal to 14 kJ mol⁻¹. However, another study by Amira et al. [17] studied the phosphoric acid acidulation of Tunisian phosphate and established that the attack rate increased with increasing temperature and the experimental results fit the shrinking-core model with an ash layer diffusion control with an activation energy equal to 25.4 ± 1.8 kJ mol⁻¹. The attack of the natural phosphates being complex, is the reason that our team initially used synthetic phosphate for the modelization of the reaction of acid attack of phosphates [5-11].

The attack reaction of a synthetic fluorapatite by phosphoric acid [5] and hydrochloric acid [6] was performed by Brahim et al. In phosphoric acid, the results showed a change of mechanism at a temperature of about 45°C. According to these authors, the low activation energy value at a temperature below 45°C suggests a diffusion phenomenon, whereas for a higher temperature the attack reaction appears to be controlled by a chemical process. Similarly, Antar et al. [8,9] examined the attack of a Fap by a mixture of sulfuric acid and phosphoric acids at different temperatures. These authors [11] reported three processes for the dissolution of phosphate rocks in a mixture of sulfuric and phosphoric acids at 25°C. These processes are the dissolution of the ore, the precipitation of calcium sulfate hemihydrate (CaSO₄·1/2H₂O:HH) and the transformation of the latter into dihydrate (CaSO₄·2H₂O:DH). In the same context, Zendah et al. [10] dissolved an asynthetic carbonate fluorapatite (CO₃-Fap) in phosphoric acid at 25–55 °C and established that the digestion is controlled by a diffusion phenomenon.

The majority of the studies published is devoted to thermodynamic and kinetic reactions and used techniques such as conductometry, ICP (Inductively Coupled Plasma) [32], isoperibolic calorimetry [33]

and microscopy [34]. These techniques do not allow the accurate tracking of the phosphate rock dissolution process with time. There are other techniques that supply more precise information about what happens in situ, such as DRC and microcalorimetry, which fewer studies have used, notably for kinetic studies.

Indeed, only some studies performed in our laboratory used these techniques [2-10]. Amira et al. [14, 17, 35] performed them on a Tunisian phosphate ore (from Gafsa) using phosphoric acid in the 25–60 °C range using a DRC. Similarly, Brahim et al. [5,6] used a C-80 SETARAM calorimeter to project the thermodynamic and kinetic aspects of the digestion of a synthetic FAP in phosphoric acid at different concentrations (10, 18 and 30% by weight of P₂O₅).

Regardless of the technique used, the yield of the reaction of the acid attack on natural phosphate is always inadequate. Indeed, the filtration of phosphogypsum is paramount to the phosphoric acid production because gypsum affects the efficiency, purity and crystallization of phosphoric acid. On the other hand, this process has some cons such as sulfate contamination in the product and the disposal of gypsum that causes soil and water pollution [36]. For this reason, the Tunisian industrial scale, Société Industrielle d'Acide Phosphorique and Engrais (SIAPE), needs to advance this production or to revise the reaction of the acid attack on natural phosphate. Our work, which is the part of an attempt to model the reaction of the acid attack of natural phosphates, is a contribution to the kinetic study of this reaction. So, in the light of these observations, this study aimed to examine the effects of kinetics parameters such as reaction temperature, acid concentration, liquid-to-solid ratio, particle size and string speed in the dissolution of Tunisian phosphate in the mixture of phosphoric and sulfuric acids solution by DRC. The aim is to meet the needs of industry to decrease the charge of production and meet augmentation of demand for phosphate products.

2. Materials and methods

The Gafsa Phosphate Company supplied the phosphate rocks used in this work which were extracted from a mine in that region. Thermogravimetry was performed using a B60 SETARAM microbalance in order to establish the chemical composition, as well as ionometry with a specific fluoride electrode ISE25F and an Ag/AgCl reference electrode and inductively coupled plasma [17].

A SETARAM model based on the differential thermal analysis which measures ΔT (the difference in temperature) between a measuring reactor and a reference one was used for the DRC. Amira et al.



studied the reliability of this method in kinetic and thermodynamic studies [17,35]. The method followed to analyze the dissolution of the NP in the sulfuric and phosphoric acid solution mixture was as follows: 100 g of the attacking solution, S, (the 100 g were composed of 20 g of concentrated H_2SO_4 and 80 g of recycled H_3PO_4 , 20% of P_2O_5) and an amount "m" of NP in a sealed sample holder to avoid contact with the attacking solution were introduced in the reactor. An equal amount of reactants was used in the reference reactor for equality. The two reagents enter into contact when the sample holder is triggered. In order to regain thermal equilibrium a certain amount of time is required, which depends on the kinetics. This is seen by the return to the base line. To calibrate the results, a power close to that produced by the chemical phenomenon studied is reproduced in the measuring cell for a variable period of time. This is also done before the NP attack. These two processes are essential to establish the specific heat of the mixture obtained before and after dissolving the NP.

3. Results and discussion

3.1 Effect of parameters

A number of tests were accomplished to observe the effect of reaction time on the dissolution of PN in the mixtures of sulfuric and phosphoric acids at different temperatures, solid/liquid ratio, concentration en mass of H_2SO_4 , stirring speed and particle size as shown in Figs.1-5. The parameters affecting the dissolution rate were carried out for each parameter using the values indicated in Table 1. While the effect of one parameter was checked, the other parameters' values indicated with asterisks in Table 1 maintained the same.

3.2 Kinetic analysis

During the kinetic investigations, the evolution of

Table 1. The ranges of the parameters used in the attack experiments

Parameters	values
Ratio « S/L »	20/100; 25/100*; 30/100; 35/100
Concentration « C » (% H_2SO_4)	20; 50; 60; 80*
Particle size « G » (μm)	63; 100; 200*; 315
Stirring speed « SS » (revolution/min)	50; 75; 100; 200*; 400
Temperature « T » ($^{\circ}C$)	25*, 30, 35, 40, 45, 50, 60

*The constant values were chosen for the case when the effect of the other parameters was studied

the acid attack reaction of the NP was followed by plotting the conversion fraction "X" as a function of time. The latter is inferred from the following equation:

$$X = Q_t / Q_{max}$$

Where Q_t is the amount of heat released at time t and Q_{max} is the amount of total heat released at the end of the reaction.

3.2.1 Effect of the reaction temperature

The effect of the reaction temperature on the rate of the attack was investigated in the 25-60 $^{\circ}C$ temperature range. Several experiments were performed with seven different reaction temperatures, plotted in Fig. 1 by dissolving around 25g of phosphate ore in 100g of mixture of sulfo-phosphoric solution. According to experimental results, it was shown that increasing reaction temperatures resulted in a decreased dissolution of NP. This observation is surprising because it is much less well-known that the rates of some reactions are retarded by increasing the temperature. The explanation of this phenomenon is rather attributed to the complication of the attacking reaction that is translated into multi-steps.

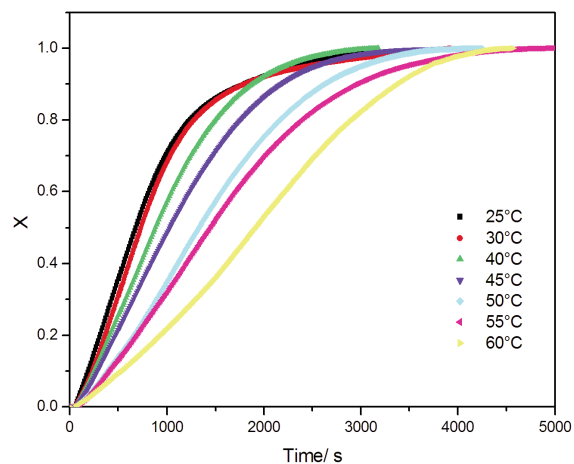


Figure 1. Variation of the conversion fraction versus time at different temperatures. (C: 96% mass H_2SO_4 ; S/L: 25/100; SS: 200 rpm; G: 80 % de NP $\leq 800 \mu m$)

3.2.2 Effect of sulfuric acid concentration

The effect of H_2SO_4 concentration on the dissolution rate was studied (15- 80% by weight of H_2SO_4). The experimental data seen in Fig. 2 indicate that the dissolution decreased with the increasing H_2SO_4 concentrations. This evidence can be elucidated by the viscosity of solution [37].



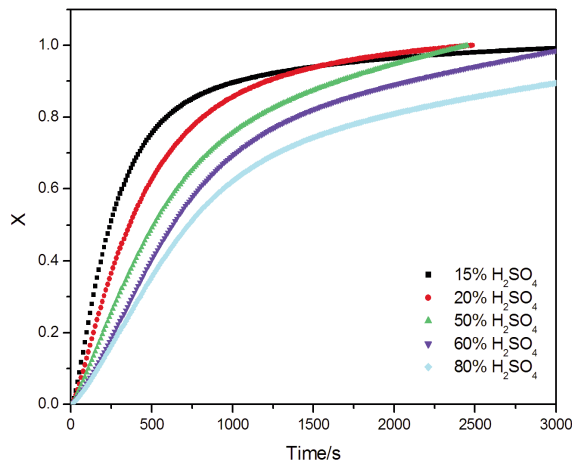


Figure 2. Variation of the conversion fraction versus time at different concentrations ($T: 25^{\circ}\text{C}$; $S/L: 25/100$; $SS: 200\text{ rpm}$; $G: 80\%$ of $NP \leq 800\ \mu\text{m}$)

3.2.3 Effect of the solid-to-liquid ratio

To look at the effect of the solid-to-liquid ratio on dissolution rate, the experiments were performed at 20/100, 25/100, 30/100, 35/100. The results shown in Fig. 3 indicate that the dissolution rate drops with a rise in the solid-to-liquid ratio. This situation can be explained by the increase in the amount of solid per amount of reagent in the reaction mixture. In the previous work [38], we showed that the attack of a phosphate ore by a mixture of sulfo-phosphoric acid solution is a complex process beginning by the dissolution of the ore and then the precipitation of the dihydrate, hemihydrate or a mixture of these two products following the values of the mass studied. The conversion fraction "X" as a function of time variation could be attributed to the variation of the proportions of the products formed in the residue at the end of the attack.

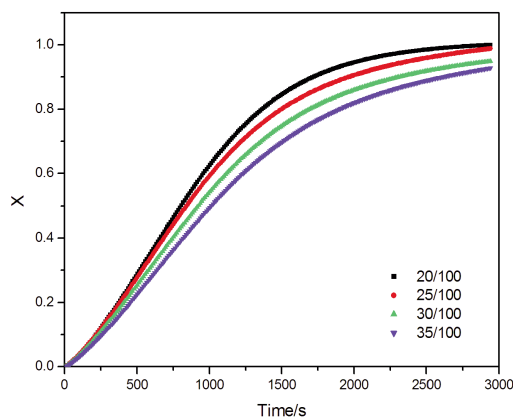


Figure 3. Variation of the conversion fraction versus time at different solid/liquid ratio ($C: 96\%$ mass H_2SO_4 ; $T: 25^{\circ}\text{C}$; $SS: 200\text{ rpm}$; $S/L: 25/100$; $G: 80\%$ de $NP \leq 800\ \mu\text{m}$)

3.2.4 Effect of particle size

Different particles size ranges of PN were chosen in order to see the particle size effect on the attack reaction. The experiments on particle size were carried out using the following size fractions (100, 160, 200, 315 and 500 μm). The results of the effect of particle size on the dissolution rate given in Fig. 4 suggest that the particle size has an important effect on the dissolution of Tunisian phosphate. It is well known that the surface of the solid becomes more available when decreasing the particle size, resulting in an increase in the efficiency of the attack process. However, our results demonstrate that the dissolution rate increases with an increase in particle size. This has been explained in the previous work [39] by the change in chemical composition of calcium carbonate to determine each granule slice. This conclusion is not remarkable since Tunisian phosphate ore is celebrated for its high reactivity due to its relatively high carbonate content.

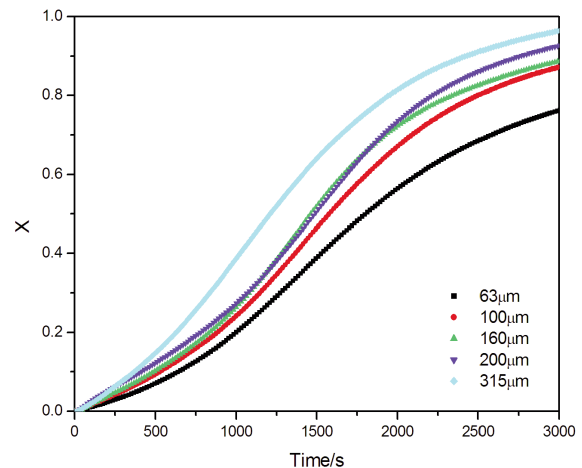


Figure 4. Variation of the conversion fraction versus time at different particle size ($C: 96\%$ mass H_2SO_4 ; $T: 25^{\circ}\text{C}$; $SS: 200\text{ rpm}$; $S/L: 25/100$)

3.2.5 Effect of Stirring Speed

Stirring speed effect on the phosphate rock dissolution process was studied for the different stirring speed 50, 75, 100, 200 and 400 rpm. However, the other parameters were fixed. The experimental results are shown in Fig. 5. This figure reveals that the stirring speed increases the dissolution rate. It means that increasing stirring rate increases the mass transfer of H^+ ions through phosphate and it dissolves faster and gives Ca ion, but these calcium ions spontaneously react with sulfate ions and so this increases the rate of the formation of gypsum crystals.

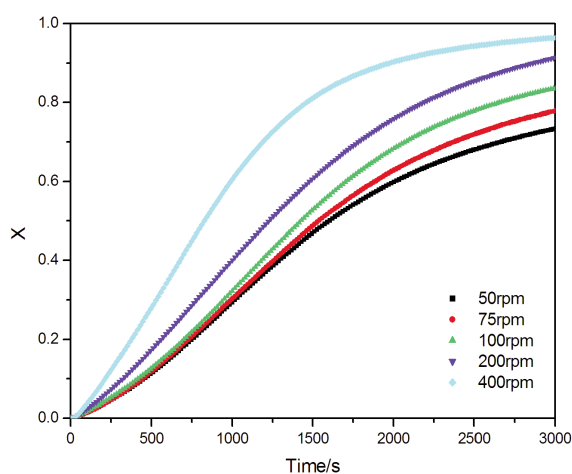


Figure 5. Variation of the conversion fraction versus time at different stirring speed (C : 96 % mass H_2SO_4 ; T : 25°C; S/L : 25/100; G : 80 % de NP $\leq 800 \mu m$)

3.3 Kinetic Model

Fluid-solid heterogeneous reactions are of a great interest for industrial applications regarding a number of chemical processes. A successful and efficient performance of chemical reactors for these processes is generally based on kinetic data. In order to determine the kinetic parameters and rate-controlling step for the dissolution of phosphate rock in a mixture of phosphoric and sulfuric acid solutions, we have considered the use of models of pseudo-homogeneous kinetics and heterogeneous kinetics. Indeed, in an earlier work carried out in our laboratory by K. Brahim [40] and K. Antar [41], the application of homogeneous kinetic models on the acid attack reaction on a natural phosphate did not lead to results.

The shrinking core model is the most crucial model suggested for the derivation of the rate expression of a noncatalytic fluid–solid reaction [42–49]. It is believed that the reaction happens on the outer surface of the solid and that this surface shrinks toward the center of the solid as the reaction proceeds. The reaction rate may be controlled by film diffusion, chemical reaction, or product layer diffusion according to this model. In the progressive conversion model, the liquid reactant is assumed to enter the solid particle and react at all times throughout the particle.

The rate of reaction between the solid particle and the dissolution agent may be controlled by one of the following three steps [44]:

- Diffusion of the fluid reactant from the main body of the fluid film to the surface of the solid

$$X = kt \quad (1)$$

- Reaction on the surface between the fluid reactant and the solid

$$[1 - (1 - X)^{\frac{1}{3}}] = kt \quad (2)$$

- Diffusion of the products of reaction from the surface of the solid through the fluid film back into the main body of the fluid.

$$[1 - 3(1 - X)^{\frac{2}{3}} + 2(1 - X)] = kt \quad (3)$$

where t is reaction time (s), X conversion rate, k is the reaction rate constant (s^{-1}). According to the literature, the latter relies on several factors such as: the solid/liquid ratio (S/L), the concentration of the acid solution (C), the particle size (G), the stirring speed (SS), and temperature (T), according to the relationship (Eq.4).

$$k = k_0 (S/L)^a C^b G^c (SS)^d \text{Exp}(-Ea/RT) \quad (4)$$

With a , b , c and d of the constants, k_0 is the rate constant and Ea is the activation energy.

In addition to the heterogeneous models, pseudo-homogeneous models can also be used to derive the rate equations for the heterogeneous reactions. In pseudo-homogeneous models, the rate equations are written as [47–49]:

$$-\ln(1 - X) = kt \begin{cases} \text{for the first-order} \\ \text{pseudo-homogeneous model} \end{cases} \quad (5)$$

$$(1 - X)^{-1} - 1 = kt \begin{cases} \text{for the second-order} \\ \text{pseudo-homogeneous model} \end{cases} \quad (6)$$

The reaction kinetics between NP and mixtures of sulfuric and phosphoric acids solutions was analyzed statistically and graphically by using the shrinking core model (Eq. 1-3), but it was concluded that the data did not fit this model. The correlation coefficient-squared (R^2) was considered as a measure of goodness of the fit. It was found that none of the models could represent the data very well as R^2 remained below 0.9 for the majority of kinetic factors. Therefore, it was determined that the heterogeneous models were inapt for this study. The data were then analyzed by using the pseudo-homogeneous models. The plots of the left side of Eq. 5 and 6 versus time must be a straight line if the dissolution follows these models. It was found that the data did not fit the second-order pseudo-homogeneous model. Using the first-order pseudo-homogeneous reaction model, the left side of Eq. 5 was plotted against the reaction time. As can be shown in the plots given in Figs. 6-10, straight lines passing through the origin were obtained and the value of the correlation coefficient is very close to 1. This proves

the good agreement between the model and the experimental measurements. Therefore, the dissolution process could be stated by a first-order pseudo-homogeneous model. In compliance with these results, the semi-empirical equation illustrating the kinetics of this process can be written as follows:

$$-\ln(1-X) = k_0 (L/S)^a C^b G^c (SS)^d \text{Exp}(-Ea/RT)t \quad (7)$$

Linear regression was used to calculate the slopes of $\ln k$ as function of against $1/T$, $\ln(C)$, $\ln(S/L)$, $\ln(G)$ and $\ln(SS)$ (Figs. 11-14). These calculations lead $a = 0.75$, $b = -0.461$, $c = 0.447$ and $d = 0.471$, suggesting a positive effect of the liquid/solid ratio, the particle size and the stirring speed, and a negative one of the acid concentration.

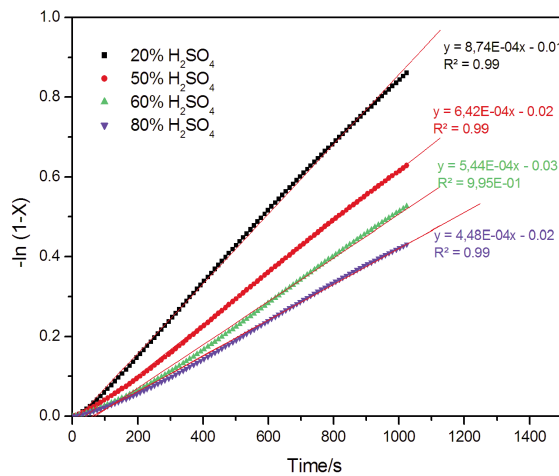


Figure 6. Graphical representation according to Eq. (6) for different acid concentration (T:25°C; S/L: 25/100; SS: 200 rpm; S/L: 25/100)

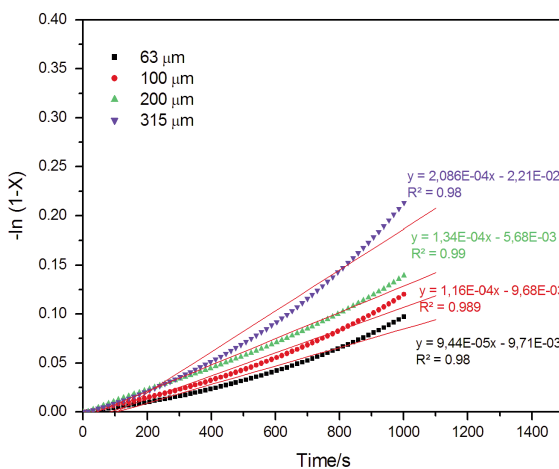


Figure 7. Graphical representation according to Eq. (6) for various particle size (C: 96 % mass H₂SO₄; T:25°C; SS: 200 rpm; S/L: 25/100)

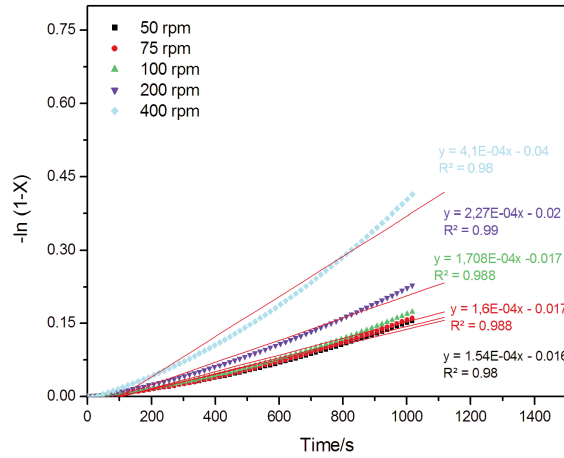


Figure 8. Graphical representation according to Eq. (6) for various speed string (C: 96 % mass H₂SO₄; T:25°C; S/L: 25/100)

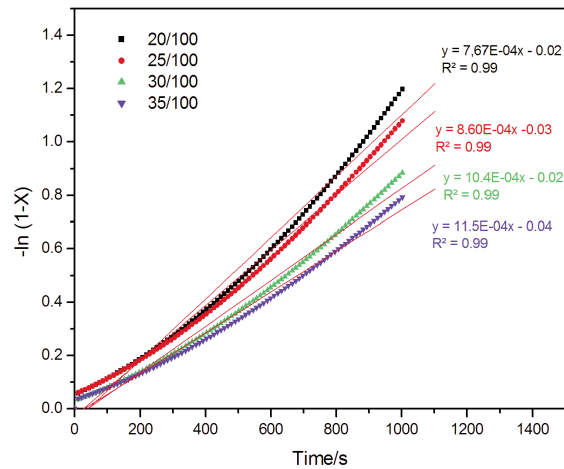


Figure 9. Graphical representation according to Eq. (6) for various solid/liquid ratios (C: 96 % mass H₂SO₄; T:25°C; SS: 200 rpm; S/L: 25/100)

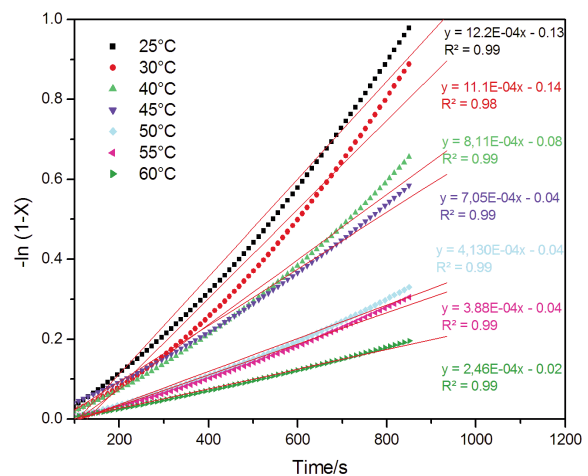


Figure 10. Graphical representation according to Eq. (3) for different temperature (C: 96 % mass H₂SO₄; S/L: 25/100; SS: 200 rpm)



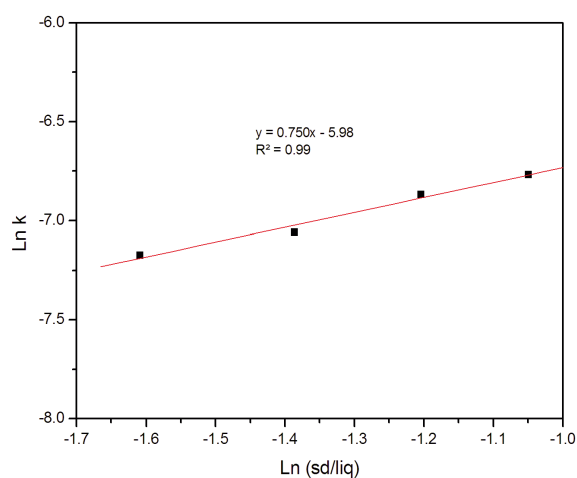


Figure 11. Determination of reaction order with respect to solid liquid ratio

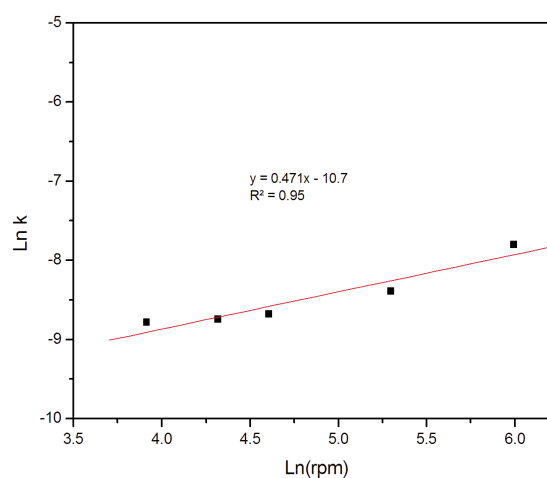


Figure 14. Determination of reaction order with respect to string speed

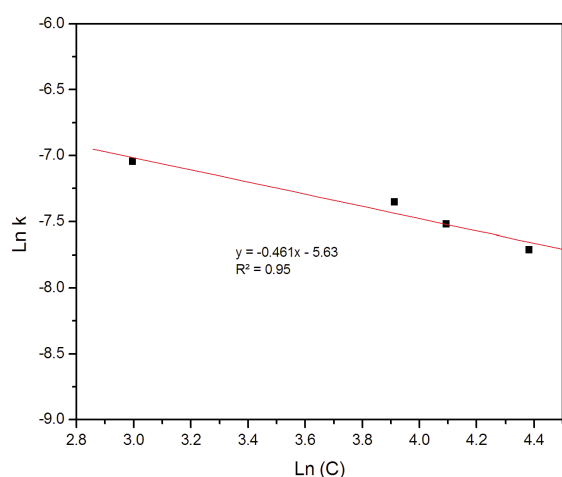


Figure 12. Determination of reaction order with respect to acid concentration

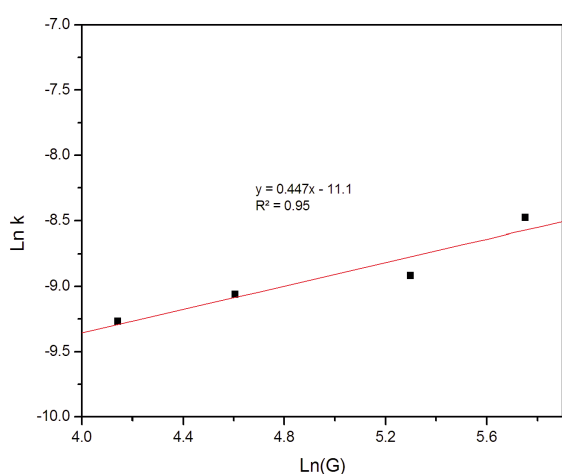


Figure 13. Determination of reaction order with respect to particle size

3.4 Activation energy

To additionally validate that the reaction of dissolution phosphate with mixtures of sulfuric and phosphoric acids solutions is controlled by first pseudo-homogeneous models, the activation energy E_a was determined using the following Arrhenius equation.

$$-\ln(1-X) = kt = A \exp(-E_a / RT) t \quad (8)$$

So

$$\ln k = \ln A - (E_a / RT) \quad (9)$$

At various reaction temperatures, using a known size range of the rock particles and the acid concentration with a specific solid/liquid ratio and speed string, the results have been plotted between the $-\ln(1-X)$ versus time t as shown in Fig.10. The values of the apparent rate constants, k , have been determined from the slopes of the straight lines.

A plot of $\ln k$ versus $1/T$ should result in a straight line with a slope of $-E_a/RT$ and an intercept of $\ln A$ if the experimental data are fitted well by the Arrhenius equation. As seen in Fig.15, two straight lines are obtained. The first region presents the variation between 25-40 °C, and the second region between 45-60°C. The apparent activation energies ($(E_a)_{app}$) for the attack of NP by mixtures of sulfuric and phosphoric acids solutions were found to be $-18.48 \text{ kJ mol}^{-1}$ for the first region and $-57.89 \text{ kJ mol}^{-1}$ for the second range.

It is well-known by most chemistry students that chemical reactions most of the time follow the

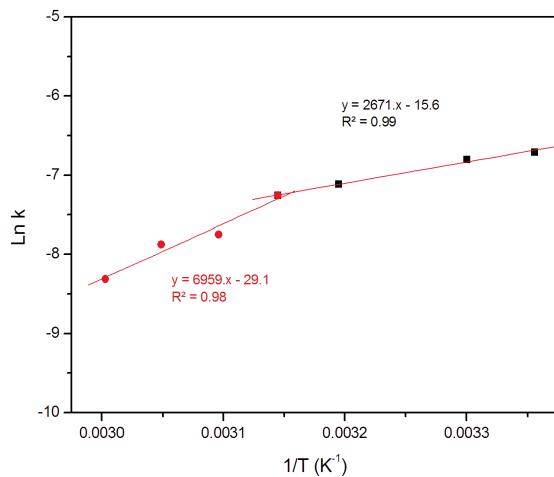


Figure 15. Arrhenius plot for the dissolution process

Arrhenius law with the positive activation energy alongside the temperature increase. It is much less well-known [50-55] that the rates of some reactions are retarded by elevated temperature and are therefore associated with negative activation energies.

Rare instances of negative activation energies have, indeed, been observed, such as our example of the dissolution the NP in the mixtures of sulfuric and phosphoric acids. Negative activation energies were predicted by Casey and Sposito [50], presented rationalizations of the activation energy of mineral dissolution, when no examples were known. In the meantime, at least three similar cases have been reported: the dissolution of stibiconite [51], the oxidative dissolution of arsenopyrite in the presence of ferric ion [50], and magnesite dissolution in slightly alkaline solution [52].

The value of activation energy in the dissolution process is characterized to identify the controlling step. The activation energy of a diffusion controlled process is typically found to be from 4-12 kJ mol⁻¹ [56], while for a chemically controlled process, it is usually reported to be greater than 40 kJ mol⁻¹ [57-58] and for product layer diffusion control; the activation energy is usually lower than 40 kJ mol⁻¹ [61-63]. The experimental results, negative values of (E_a)_{app}, are most explained by a sequel of reactions that contain a step where one reaction path is dominant at all temperatures while the less energetic side reaction produces an inhibitor of the rate-limiting step [52]. The dissolution of phosphate rock in acid mixture is a complicated phenomenon in the region temperature of 25-60°C. This observation is confirmed below by the application of an isoconversional model.

Miller [64], Mackinnon and Ingraham [65] reported that a change in the variation energy was probably a result of the alteration in the reaction mechanism. It may be assumed that two consecutive

processes control the rate. In another study, the earlier results by Brahim et al [5], of the attack reaction of a synthetic phosphate (FAP) by phosphoric acid highlighted rather a mechanism change at a temperature around 45 °C. The low value of activation energy, equals about 20 kJ mol⁻¹, below 45°C suggests a diffusion phenomenon, while for a higher temperature (E_a = 101 kJ mol⁻¹) the attack reaction seems to be regulated by a chemical process. In this case, the attack followed a two or one step mechanism depending on the temperature range. Similar results were observed by Souza et al. [62] and Abdel-Aalal [58]. The results show a change in the leaching phenomena of calcareous material after about 45 °C, a situation that may be attributed to the mixed chemically-diffusion controlled behavior of the reaction process.

The experimental data were tested using a graphical method and it was established that the kinetic expression including the parameters for two different temperatures used in this dissolution process can be written as:

$$-\ln(1-x) = [2,2E - 09((S/L)^{0.75} C^{-0.461} G^{0.447} (SS)^{0.471} \exp(2671/T))t]. T \leq 40^\circ\text{C} \quad (9)$$

$$-\ln(1-x) = [2,2E - 09((S/L)^{0.75} C^{-0.461} G^{0.447} (SS)^{0.471} \exp(6959/T))t]. T > 45^\circ\text{C} \quad (10)$$

To examine the workability and to appraise the applicability of the suggested model, calculated (X_{Theor}) and experimental conversion (X_{expl}) data were plotted in (Fig. 16). It is observed that the agreement between the experimental and the calculated values is very good, with a correlation coefficient of 0.97. On the other hand, the data in the scatter diagram point out a positive trend to regroup around the regression line; this dispersion shows a good relationship between the variables involved.

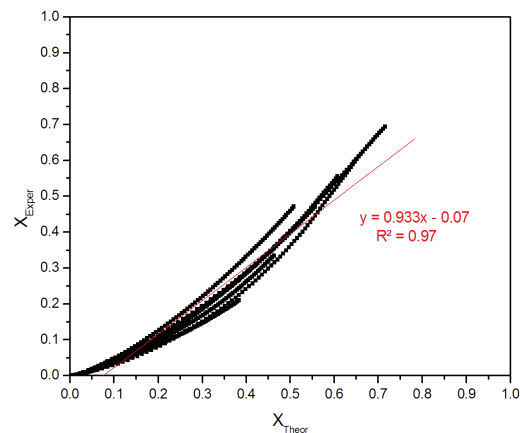


Figure 16. Agreement between experimental and calculated conversion values



3.5 Isoconversional model

To compare the suggested model and to monitor the variation of the activation energy as a function of the decomposition rate of the NP during the same experiment, the isoconversional model was used. In fact, the latter is a powerful source of information for the determination of the kinetic scheme of a complex process. So it associates the shift in the mechanism to a variation of activation energy with the conversion degree [66]. According to that model, the converted fraction of a reactant is expressed as a function of time by the equation:

$$d\alpha / dt = kf(\alpha) \quad (11)$$

Where, k is the rate constant and $f(\alpha)$ a mathematical function associated to the mechanism.

The integration of Eq. 11 leads to:

$$g(\alpha) = \int_0^{\alpha} d\alpha / f(\alpha) = kt \quad (12)$$

Using the Arrhenius law equation, Eq. 12 can be transformed into:

$$\ln(t) = Ea / RT + \ln(g(\alpha) / A) \quad (13)$$

At a certain conversion rate, $\ln(g(\alpha)/A)$ is constant, and thus it is possible to determine the activation energy, whatever the mechanism, by plotting $\ln(t)$ versus $1/T$ [67]. The examples of plots of $\ln(t)$ versus $1/T$ are shown in Fig.17.

Fig.18 presents the variation of activation energies as a function conversion fraction according to the isoconversional model. We can notice a large variation of the whole activation energy suggesting a reaction mechanism that is composed of several steps [68] and verified the complexity of the NP attack acid reaction.

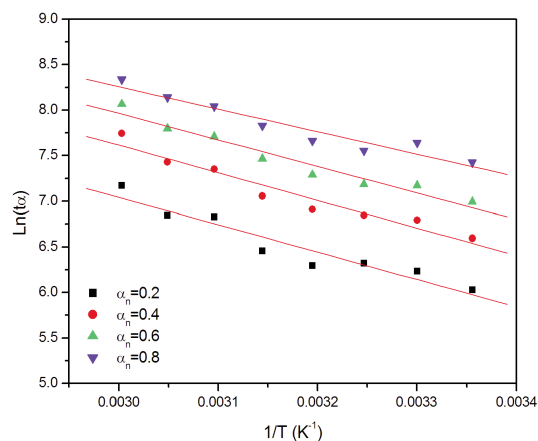


Figure 17. Examples of plots of $\ln(t)$ versus $1/T$ for $25 \leq T \leq 60^\circ\text{C}$ at different X

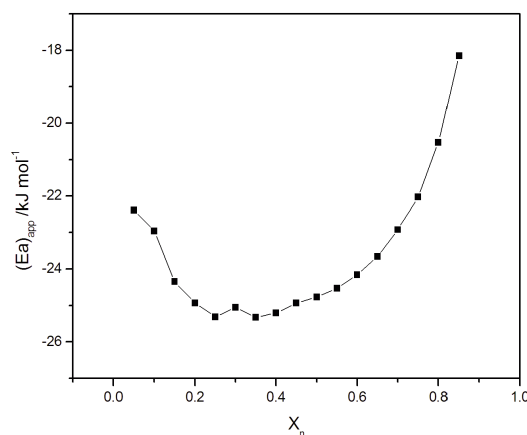


Figure 18. Dependence of the activation energy versus the conversion fraction according to the isoconversional model

4. Conclusions

The present study has clarified the dissolution process of NP and a mixture of sulfuric and phosphoric acids. Based on the results obtained in this research, the following conclusions can be drawn:

- The experimental results uncovered that the dissolution rate decreased with increasing solution concentration, reaction temperature and solid/liquid ratio, and increasing particle size and string speed.

- Analysis of the kinetic data by different kinetic models indicates that the attack of phosphate rock with a mixture of sulfuric and phosphoric acid is governed by the first pseudo-homogenous model.

- The graphical and statistical methods utilized in the kinetic models provided attack kinetics of PN in a mixture of sulfuric and phosphoric acid, which was described by the first-order pseudo-homogenous reaction control model. The apparent activation energy for dissolution was found to be $-18.48 \text{ kJ mol}^{-1}$ for the region $25-40^\circ\text{C}$ and $-57.89 \text{ kJ mol}^{-1}$ for the range $45-60^\circ\text{C}$. A semi-empirical mathematical model was formulated.

- The isoconversional model shows a large variation of the whole activation energy suggesting a multi-step process and verifies the negative value of apparent activation energies (complexity of the NP attack with a mixture of sulfuric and phosphoric acids reaction)

References

- [1] P. Becker, Phosphates and Phosphoric Acid. Marcel Dekker (1989).
- [2] L. Visima, M. Veinderma, Anal Sci., 7 (1991) 1161-1163.
- [3] U.S. Geological Survey, 2014, Phosphate rock statistics, in Kelly, T.D., Matos, G.R., comps., Historical statistics for mineral and material



- commodities in the United States: U.S. Geological Survey Data Series 140, accessed [August 2014].
- [4] N. Kanari, N. Menadb, F. Diota, E. Allaina, J. Yvona, J. Min. Metall. Sect. B-Metall., 52 (2016) 17-24
- [5] K. Brahim, K. Antar, I. Khattech, M. Jemal, Sci. Res. Essays., 3 (2008) 35-39.
- [6] K. Brahim, I. Khattech, J.P. Dubés, M. Jemal, Thermochim. Acta., 436 (2005) 43-50.
- [7] K. Brahim, A. S. Baatout, I. Khattech, M. Jemal, J. Therm. Anal. Calorim., (2017) 6221-8.
- [8] K. Antar, K. Brahim, M. Jemal, Thermochim. Acta., 449 (2006) 35-41.
- [9] K. Antar, M. Jemal, Thermochim. Acta., 452 (2007) 71-75.
- [10] H. Zendah, I. Khattech, M. Jemal, Thermochim. Acta., 565 (2013) 46-51.
- [11] M. W. Guidry, F. T. Mackenzie, Geochim. Cosmochim. Acta., 67 (2003) 2949-2963
- [12] S. V. Dorozhkin, Colloid. Interface. Sci., 191 (1997) 489-497
- [13] K. Antar, M. Jemal, Thermochim. Acta., 474 (2008) 32-35
- [14] A. S. Baatout, K. Brahim, I. Khattech, L. Kamoun, M. Jemal, J. Therm. Anal. Calorim., (2016) 6825-z.
- [15] A. Chaabouni, C. Chtara, A. Nzihou, H. El-Feki, Adv. Chem., 6 (2013) 908-913.
- [16] F. Ben Brahim, M. Mgaidi, M. El Maaoui, Can. J. Chem. Eng., 77 (1999) 136-142.
- [17] B.S. Amira, K. Ibrahim, I. Khattech, M. Jemal, Therm. Anal. Calorim., 124 (2016) 1671-1678.
- [18] M. Ashraf, Z. Iqbal-Zafar, T. Ansari, Hydrometallurgy., 80 (2005) 286-292.
- [19] M. Gharabaghi, M. Irannajad, M. Noaparast, Hydrometallurgy., 103 (2010) 96-107.
- [20] H. F. Aly, M.M. Ali, M.H. Taha, Arab. J. Nucl. Sci. Appl., 46 (2013) 1-16.
- [21] E. O. Olenipekun, Bull. Chem. Soc. Ethiop., 13 (1999) 63-70.
- [22] M. Sınırkaya, A.K. Özerand M.Ş. Gülaboğlu, Pamukkale. Univ. Muh. Bilim. Derg., 20 (2014) 253-257.
- [23] C. E. Calmanovici, B. Gilot, C. Laguerie, Braz. J. Chem. Eng., 14 (1997) 95-102.
- [24] F. Sevim, H. Saraçand A. Yartasi, Ind. Eng., 42 (2003) 2052-2057.
- [25] M. Lassis, A. Mizane, N. Dadda, R. Rehamnia, Environ. Nanotechnol. Monit. Manage., 4 (2015) 12-16
- [26] A. Mizane and A. Louhi, Asian. J. Chem., 20 (2008) 711-717.
- [27] T.F. Fariss, S.S.E.H. Elnashaie, S.M. Abdel-Razik, F. A. Abdel-Aleem and H.A. Ibrahim. Fert. Res., 29 (1991) 209-227.
- [28] A. Mizane, A. Louhi, Eng. Appl. Sci., 2 (2007) 1016-1019.
- [29] R.L. Gilbert, E. C. Moreno, Ind. Eng. Chem. Process. Des. Dev., 4 (1965) 368-371.
- [30] M. Jamialahmadi, S.H. Emam, Dev. Chem. Eng. Mineral. Process., 6 (1998) 273-293.
- [31] N. Frikha, A. Hmerchaand S. Gabsi, Can. J. Chem. Eng., 92 (2014) 1829-1838.
- [32] S. V. Sluis, Y. Meszaros, M. Gerda, V. Rosmalen, Ind. Eng. Chem. Res., 26 (1987) 2501-2505.
- [33] E.O. Huffmann, W.E. Cate, M.E. Deming, K. Elmore, Agric. Food. Chem., 5 (1957) 266-275.
- [34] S. V. Dorozhkin, J. Prakt. Chem., 338 (1996) 620-626.
- [35] A.S. Baatout, M. Hichri, A. Bechrifa, I. Khattech, Thermochimica. Acta., 580 (2014) 85-92.
- [36] J. Mulopo, D. Ikhu-Omoregbe, Chem. Eng. Process. Technol., (2012).
- [37] S.V. Sluis, Y. Meszaros, W.G.J. Marchee, H.A. Wesselingh, G.M.V. Rosmalen, Ind. Eng. Chem. Res., 26 (1987) 2501-2505.
- [38] L.Z. Olfa, B. Khemaies, B.M. Feten, K. Ismail, Adv. Mater. Phys. Chem (ampc), 8(2018) 411-427.
- [39] L.Z. Olfa, B. Khemaies, B.M. Feten, K. Ismail, Advances in Materials Physics and Chemistry, 8(2018) 429-440.
- [40] K. Brahim, Contribution à l'étude thermodynamique et cinétique de l'attaque phosphorique d'une fluorapatite Application à un phosphate naturel thèse de doctorat. Université Tunis el Manar, Tunisie (2006).
- [41] K. Antar, Contribution à l'étude thermodynamique et cinétique de l'attaque sulfophosphorique d'une fluorapatite Application à un phosphate naturel thèse de doctorat. Université Tunis el Manar, Tunisie (2008).
- [42] O. Levenspiel, Chemical reaction Engineering, Third ed., John Wiley and Sons: New York, (1999) pp. 566-586.
- [43] Q. Feng, S. Wen, Y. Wang, W. Zhao, J. Liu, Bull. Korean Chem. Soc., 36 (2015) 1100-1107.
- [44] N. Demirkiran, A. Künkül, Theor. Found. Chem. Eng., 45 (2015) 114-119.
- [45] E. A. Abdel-Aal, M. M. Rashad; Kinetic study on the leaching of spent nickel oxide catalyst with sulfuric acid. Hydrometallurgy., 74 (2004) 189-194.
- [46] E. A. Abdel-Aal, Leaching kinetics of gibbsitic bauxite with sodium hydroxide, E3S Web of Conferences 8, 01021, (2016).
- [47] G.U.R. Aycan, Korean. Chem. Eng., 24 (2007) 588-591
- [48] M.E. Arzutu, M.M. Kocakerim, M. Çopur, Ind. Eng. Chem. Res., 43 (2004) 4118-4123.
- [49] O. Levenspiel, Chemical Reaction Engineering, New York: Wiley 1972.
- [50] W.H. Casey, G. Sposito, Geochim. Cosmochim. Acta., 56 (1992) 3825-3830.
- [51] M. Biver, Some Kinetic Aspects of the Mobilization of Antimony from Natural Sources, Ruprecht-Karls-Universität Heidelberg, Luxemburg 2011.
- [52] J. D. Rimstidt, J.A. Chermak, P.M. Gagen, In Environmental Geochemistry of Sulfide Oxidation, ACS Symposium Series 550 (eds. C.N. Alpers, D.W. Blowes) American Chemical Society, Washington, chapter 1. (1993).
- [53] G.D. Saldi, J. Schott, O.S. Pokrovsky, E. Oelkers, Geochim. Cosmochim. Acta., 74 (2010) 6344-6356.
- [54] Y. Abali, S. Colak, A. Yarstri, Hydrometallurgy., 46 (1997) 13-25.
- [55] A. Yarstri, M. Kocakerim, S. Yapici, C. Ozmetin, Ind. Eng. Chem. Res., 33 (1994) 2220-2225.
- [56] N. Demirkiran, Hydrometallurgy., 95 (2009) 198-202.
- [57] Z. Ouyang, Y.F. Chen, S.Y. Tian, L. Xiao, C.B. Tang, Y. J. Hu, Z. M. Xia, Y.M. Chen, L.G. Ye, J. Min. Metall. Sect. B-Metall., 54 (2018) 411-418.



- [58] E. A. Abdel-Aal, Hydrometallurgy., 55 (2000) 247–254
- [59] E.O. Olanipekun, Hydrometallurgy., 53(1999) 1-10.
- [60] A. A. Baba, F. A. Adekola, A. O. Folashade. Appl. Sc. Environ. Mgt., 9 (2005) 15-20.
- [61] M.M. Antonijevic, Z.D. Jankoric, M.D. Dimitrijevic, Hydrometallurgy., 11(2004)329-334.
- [62] A. D. Souza, P. S. Pina, V. A. Leao, C.A. Silva, P. F. Siqueira, Hydrometallurgy., 89 (2007) 72–81.
- [63] Z.I. Zafar, M. Ashraf, Chem. Eng., 131 (2007) 41–48.
- [64] J. D. Miller, Miner. Sci. Eng., 5 (1973) 242-254.
- [65] D.J. MacKinnon, T.R. Ingraham, Can. Metall. Q., 9 (1970) 444-448.
- [66] M. G. Fertani, M. Jemal, J. Therm. Anal. Calorim., (2015) 4980-7.
- [67] N. Sbirrazzuoli, D. Brunel, L. Elegant, J. Therm. Anal. Calorim., 38 (1992)1509–1524.
- [68] S. Vyazovkin, Comput. Chem., 18 (1997) 393–402.

RASTVARANJE FOSFATNE RUDE IZ TUNISA MEŠAVINOM SUMPORNE I FOSFORNE KISELINE: ISPITIVANJE KINETIKE UZ POMOĆ DIFERENCIJALNE REAKCIJSKE KALORIMETRIJE

O. Lachkar-Zamouri ^a, K. Brahim ^{a*}, F. Bennour^b, I. Khattech ^a

^{a*} Odsek za hemiju: Laboratorija za LR15ES01 materijale, kristalohemiju i primenjenu termodinamiku, Univerzitet El Manar, Tunis

^b Uprava za naučna istraživanja, Tuniska hemijska grupa, Sfax, Tunis

Apstrakt

Mešavina fosforne i sumporne kiseline je korišćena da bi se istražila kinetika rastvaranja rude fosfata pomoću diferencijalne reakcijske kalorimetrije. Ispitivan je uticaj čvrsto-tečnog odnosa, koncentracije, brzine mešanja, veličine čestica, i temperature reakcije. Ustanovljeno je da se stopa rastvaranja povećavala sa povećanjem brzine mešanja i veličine čestica. Ipak, povećanje čvrsto-tečnog odnosa, temperature i koncentracije je smanjilo stopu rastvaranja. Ustanovljeno je da se stopa rastvaranja može predstaviti modelom pseudo-homogene reakcije prvog reda. Dve negativne vrednosti prividne energije aktivacije nađene su u rasponu od 25 do 60°C. Eksperimentalni podaci su testirani grafičkim i statističkim metodama. Utvrđeno je da sledeći modeli najviše odgovaraju eksperimentalnim podacima i kreirana je empirijska jednačina za taj proces.

$$-\ln(1-x) = [2,2 E-09((S/L)0.75C -0.461G0.447(SS) 0.471exp(2671/T))]t. T \leq 40^\circ C$$

$$-\ln(1-x) = [2,2 E-09((S/L)0.75C -0.461G0.447(SS) 0.471exp(6959/T))]t. T > 45^\circ C$$

Ključne reči: Kinetika; Fosfatna ruda; Diferencijalna reakcijska kalorimetrija; Model smanjenja jezgra; Energija aktivacije; Izokonverzioni model.

